UDK 669.24:621.941:519.233.4
Original scientific article/Izvirni znanstveni članek

ISSN 1580-2949
MTAEC9, 48(2)249(2014)

OPTIMIZATION OF THE TURNING PARAMETERS FOR THE CUTTING FORCES IN THE HASTELLOY X SUPERALLOY BASED ON THE TAGUCHI METHOD

OPTIMIRANJE SIL ODREZAVANJA S TAGUCHIJEVO METODO PRI STRUŽENJU SUPERZLITINE HASTELLOY X

Abdullah Altin

Van Vocational School of Higher Education, Yuzuncu Yıl University, 65080 Van, Turkey
aaltin@yyu.edu.tr

Prejem rokopisa – received: 2013-04-23; sprejem za objavo – accepted for publication: 2013-06-11

In this study the effects of the cutting-tool coating material and cutting speed on the cutting forces and surface roughness were determined using the Taguchi experimental design. For this purpose, the nickel-based superalloy Hastelloy X was machined under dry cutting conditions with three different cemented-carbide tools. The main cutting force, F_z, is considered to be the cutting force as a criterion. The mechanical loading and the abrasiveness of the carbide particles have an increasing effect on the cutting forces. According to the results of the analysis of variance (ANOVA), the effect of the cutting speeds was not important. Depending on the tool-coating material, the lowest main cutting force was found to be 538 N and the lowest average surface roughness, 0.755 μm, both at 100 m/min with a multicoated cemented-carbide insert KC9240, whose top layer is coated by TiN. Moreover, the experimental results indicated that the CVD cutting tools performed better than the PVD and the uncoated cutting tools when turning the Hastelloy X in terms of the surface quality and the cutting forces with the current parameters.

Keywords: machinability, Hastelloy X, superalloy, cutting force, surface quality

V tej študiji so s Taguchijevim eksperimentalnim sestavom določeni vplivi materiala oplaščenega rezilnega orodja, hitrosti rezanja na silo odrezavanja in hrapavost površine. V ta namen je bila superzlitina na osnovi niklja Hastelloy X obdelana pri suhih razmerah s tremi različnimi orodji iz karbidne trdine. Kot merilo je bila vzeta glavna sila rezanja F_z. Mehansko obremenjevanje in abrazivnost karbidnih delcev vplivata na povečevanje sile pri odrezavanju. Skladno z rezultati analize variance (ANOVA) vpliv hitrosti odrezavanja ni bil pomemben. Odvisno od prevleke na rezalnem orodju je bila ugotovljena najmanjša strižna sila 538 N in najmanjša povprečna hrapavost (0,755 μm), oboje pri 100 m/min z večplastnim nanosom na vložku iz karbidne trdine KC9240 z vrhnjim prekritjem iz TiN. Rezultati poskusov so pokazali, da je pri struženju Hastelloy X s stališča kvalitete površine, sil pri rezanju pri danih parametrih CVD rezilno orodje boljše od PVD in od orodja brez prevlek.

Ključne besede: obdelovalnost, Hastelloy X, superzlitina, sile rezanja, kvaliteta površine

1 INTRODUCTION

Nickel-based alloys constitute an important class of materials that are used under demanding conditions of high corrosion resistance and high-temperature strength. These characteristics together with their good ductility and ease of cold working make them generally very attractive for a wide variety of applications; nearly all of which exploit their corrosion resistance in atmospheric, salt water and various acidic and alkaline media.[1] Hastelloy X is a nickel-chromium-iron-molybdenum alloy that has been developed for high-temperature applications and is derived from the strengthening particles, Ni_2(Mo, Cr), which are formed after a two-step age-hardening heat-treatment process. With their face-centred cubic (FCC) structure, the Ni-Cr-Mo-W alloys, known as Hastelloys, are used for marine engineering, chemical and hydrocarbon processing equipment, valves, pumps, sensors and heat exchangers.[2] Hastelloy X is chosen by many for use in furnace applications because it has an unusual resistance to oxidizing, reducing, and neutral atmospheres. The resistance to localized corrosion makes the alloy an attractive material as a general-purpose filler metal, or weld overlay.[3] Hastelloy X is widely used in the clamshell of a rocket, engine tailpipes, afterburner components, cabin heaters, and other aircraft parts.[4] It has also been found to be resistant in petrochemical applications. Hastelloy X is widely used in a number of industries.[5] Wang,[6] Richards and Aspinwall,[7] Ezugwu and Wang,[8] with Khamsehzadeh[9] studied the effect of applied stress and temperatures generated at the cutting edge and they were found to influence the wear rate and, hence, the tool life. Notching at the tool nose and the depth of cutting region was a prominent failure mode when machining nickel-based alloys. This is due to a combination of high temperature, high workpiece strength, work hardening and abrasive chips. Kramer and Hartung,[10,11] observed that cemented-carbide tools used for machining nickel-based alloys at a cutting speed of 30 m/min failed due to the thermal softening of the cobalt binder phase and the subsequent plastic deformation of the cutting edge. Focke et al.[12] examined worn tools, which revealed a layer of "disturbed material" beneath the crater and the cutting edge. Hastelloy is a registered trademark name of Haynes International Inc. The Hastelloy trademark is applied as a prefix for a range of corrosion-resistant nickel-based alloys

promoted under the name "superalloys" or "high-performance alloys". Within corrosion applications, Hastelloy alloys may be chosen as a trade-off between performance, cost and other technical issues, e.g., suitability for welding. Hastelloy alloys are generally less attractive for use in acids compared to Tantaline (Tantaline is recognized as the leading performance/price option).

Nomenclature	
v	cutting speed (m/min)
f	feed (mm/r)
d_a	axial depth (mm)
y	tool life (min)
F_m	feed (mm/min)
TL	total length

2 MATERIALS AND METHOD

2.1 Experiment Specimens

Specimens of Hastelloy X, which has an industrial usage, were prepared with dimensions of diameter Ø2 × 40 inches and then used for the experiments. The chemical composition and mechanical properties of the specimens are given in **Tables 1** and **2,** respectively. As the contents of the workpiece, chromium (21 %) and molybdenum (17 %), are high, the material is hard to machine. The material consists of approximately 50 % nickel, making the alloy suitable for high-temperature applications. The specimen was annealed and has a hardness of Rockwell B 90.

2.2 Machine Tool and Measuring Instrument of Cutting Forces

The machining tests were carried out on a JOHN-FORD T35 industrial-type CNC lathe with a maximum power of 10 kW and a rotating speed between 50 r/min and 3500 r/min. During the dry cutting process, a Kistler brand 9257 B-type three-component piezoelectric dynamometer under a tool holder with an appropriate load amplifier was used for measuring three orthogonal cutting forces (F_x, F_y, F_z). This allows direct and continuous recording and a simultaneous graphical visualization of the three cutting forces. The technical properties of the dynamometer and a schematic figure of the experimental setup are given in **Table 3** and **Figure 1**, respectively.

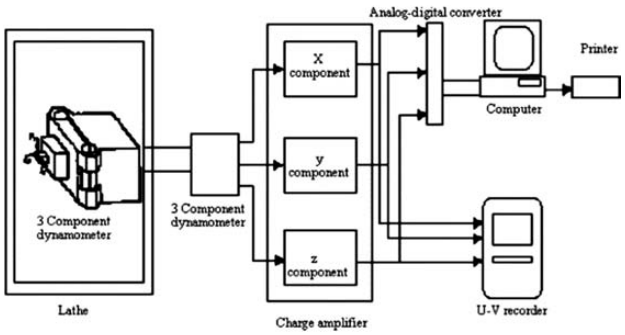

Figure 1: Measurement of the cutting forces and a schematic figure of the dynamometer unit

Slika 1: Merjenje sil pri rezanju in shematski prikaz dinamometrske enote

Table 1: Chemical composition of the workpiece material (Hastelloy X), *w*/%

Tabela 1: Kemijska sestava obdelovanca (Hastelloy X), *w*/%

Ni	Cr	Mo	Fe	Co	W	Mn	Al	Si	C	B
50	21	17	2	1	1	0.80	0.50	0.08	0.01	0.01

Table 2: Mechanical properties of Hastelloy X

Tabela 2: Mehanske lastnosti Hastelloy X

Hardness conductivity(HB)	Tensile strength (MPa)	Yield strength (MPa)	Breaking extension % (5 do)	Thermal (W/m K)
388	1370	1170	23.3	11.4

Table 3: Technical properties of dynamometer

Tabela 3: Tehnične lastnosti dinamometra

Force interval (F_x, F_y, F_z)	-5…10 kN
Reaction	< 0.01 N
Accuracy F_x, F_y	≈ 7.5 pC/N
Accuracy F_z	≈ 3.5 pC/N
Natural frequency $f_0(x, y, z)$	3.5 kHz
Working temperature	0…70 °C
Capacitance	220 pF
Insulation resistance at 20 °C	> 1013 Ω
Grounding insulation	> 108 Ω
Mass	7.3 kg

2.3 Cutting Parameters, Cutting Tool and Tool Holder

The cutting speeds (50, 65, 80, and 100) m/min were chosen by taking into consideration the ISO 3685 standard, as recommended by the manufacturers. The depth of the cut (1.5 mm) and the constant feed rate (0.10–0.15 mm/r) were chosen to be constant. During the cutting process, the machining tests were conducted with three different cemented-carbide tools, i.e., Physical Vapour Deposition (PVD) coated with TiN/TiCN/TiN; Chemical Vapour Deposition (CVD) coated with TiN+AL_2O_3-TiCN+TiN; and WC/CO. The dimensions of the test specimens were 2 × 40 inches in terms of diameter and length. The properties of the cutting tools and the level of the independent variables are given in **Tables 4** and **5**. Surtrasonic 3-P measuring equipment was used for the measurement of the surface roughness. The measurement processes were carried out with three replications. For measuring the surface roughness on the workpiece during machining, the cut-off and sampling length were considered as 0.8 mm and 2.5 mm, respectively. The ambient temperature was (20 ± 1) °C. The resultant cutting force was calculated to evaluate the machining performance. The following are the details of the tool geometry CNMG inserts when mounted on the tool holder: (a) CNMG shape; (b) axial rake angle, 6°;

Table 4: Properties of the cutting tools
Tabela 4: Lastnosti rezilnih orodij

Coating material (top layer)	Coating method and layers	ISO grade of material (grade)	Geometric form	Manufacturer and code
TiN	CVD (TiN, Al2O3, TiCN, TiN, WC)	P25-40, M20-30	CNMG120404RP	Kennametal KC9240
TiN	PVD (TiN, TiCN, TiN, WC)	P25-40, M20-30	CNMG120404FN	Kennametal KT315
WC-CO	Uncoated	P25-40, M20-30	CNMG120404MS	Kennametal K313

(c) end relief angle, 5°; and (d) sharp cutting edge. The cutting tool was mounted in the tool holder (PCLNR 2525M12) and used for such cutting tools (CNMG 120404) with an approach angle of 75°. Analysis of variance (ANOVA) was applied to the experimental study.

Table 5: Level of independent variables
Tabela 5: Nivoji neodvisnih spremenljivk

Variables	Level of variables			
	Lower	Low	Medium	High
Cutting speed, v/(m/min)	50	65	80	100
Feed, f/(mm/r)	0.1–0.15	0.1–0.15	0.1–0.15	0.1–0.15
Axial depth, d_a/mm	1.5	1.5	1.5	1.5

3 RESULTS AND DISCUSSION

3.1 Cutting forces and surface roughness

After the test specimens were prepared for experimental purposes, they were measured with a three-component piezoelectric dynamometer to obtain the main cutting force. According to **Figure 2**, increasing the cutting speed decreases the main cutting force, excluding the area between 80 m/min and 100 m/min for K313. The lowest obtained values for the main cutting force at the cutting speeds of 50 m/min, 662 N, 65 m/min, 622 N, 80 m/min, 601 N, and 100 m/min, 538 N at a 0.1 mm/r constant feed rate, respectively. The lowest main cutting force was observed at 100 m/min cutting speed as 538 N. In **Figure 2** the main cutting force depending on the cutting speed and the uncoating material of the cutting tool were changed in all the experiments. The cutting forces and surface roughness according to the experimental cutting parameters are given in **Table 6**. According to W. Konig, the cutting speed must be increased in order to reduce the main cutting forces.[13] However, in this study, a decrease was observed in the main cutting force between 50 m/min and 100 m/min. It is thought that this case is caused by the good performance of the cutting tool. The effect of the TiN-coated carbide inserts was found to be important for the main cutting force, but the effect of the cutting speeds was not important in the analysis of variance. The main cutting force decreases in spite of increasing the cutting speed from 50 m/min to 100 m/min. As a result of the experimental data, an increase of 100 % in the cutting speed (from 50 m/min to 100 m/min), a decrease in the main cutting force with K313 (6.5 %), KT315 (10 %) and KC9240 (19 %) was found with the 0.1 mm/r constant feed rate, and the decreasing contact surface area caused the main cutting force to decrease in comparison to the increased cutting speed. The decrement of the cutting force depends on the material type, the working conditions and the cutting speed range.[14] The high temperature for the flow region and the decreasing contact area and chip thickness cause the cutting force to decrease, depending on the cutting speed.[15]

As is widely known, the cutting speed must be decreased to improve the average surface roughness.[16] The scatter plot between the surface roughness and the cutting speed as shown in **Figure 3** indicated that there was a linear relationship between the surface roughness and the cutting speed. The results of **Figure 3** show that the average surface roughness decreases by 66 % with an increasing cutting speed from 50 m/min to 100 m/min

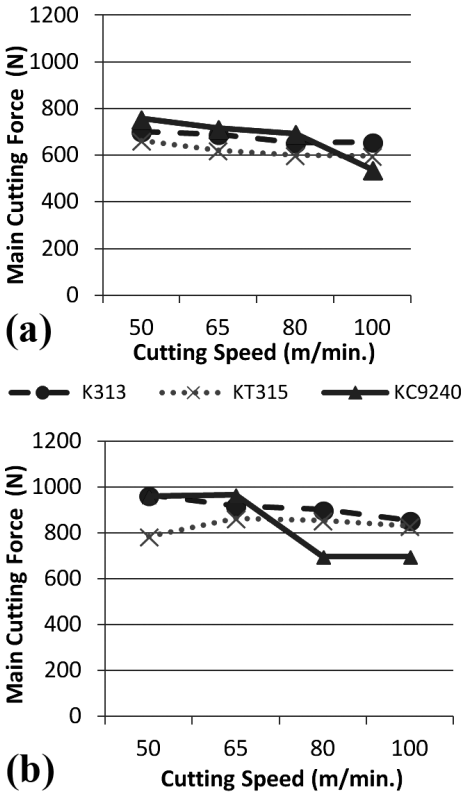

Figure 2: Change of main cutting force in Hastelloy X, according to the cutting speed: a) at f = 0.1 mm/r, b) at f = 0.15 mm/r
Slika 2: Spreminjanje glavne sile rezanja materiala Hastelloy X pri hitrostih rezanja: a) f = 0,1 mm/r in b) f = 0,15 mm/r

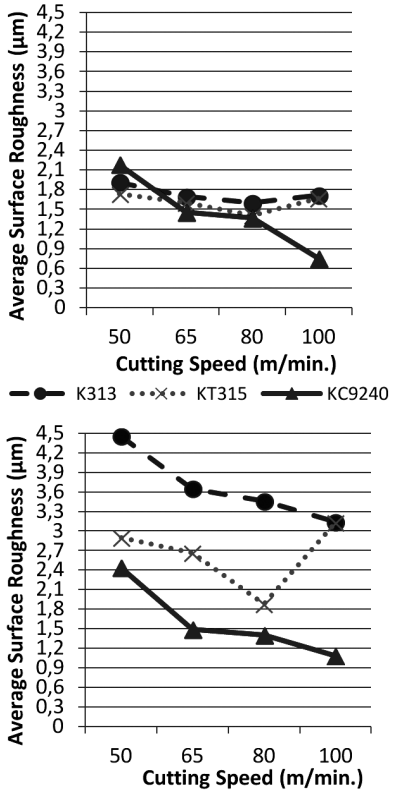

Figure 3: According to cutting speed the change of the average surface roughness in Hastelloy X: a) at f = 0.1 mm/r, b) at f = 0.15 mm/r

Slika 3: Spreminjanje povprečne hrapavosti Hastelloya X od hitrosti rezanja: a) pri f = 0,1 mm/r in b) pri f = 0,15 mm/r

Table 6: Cutting forces and surface roughness according to the experimental cutting parameters when turning Hastelloy X

Tabela 6: Sile rezanja in hrapavost površine pri ustreznih parametrih poskusa rezanja pri struženju Hastelloy X

Experiment number	Cutting tool	Cutting speed (m/min)	Feed rate (mm/r)	Depth of cut (mm)	F_x/N	F_y/N	F_z/N	R_a/µm
1	K313	65	0.1	1.5	366	75	691	1.7
2	K313	80	0.1	1.5	323	67	655	1.599
3	K313	100	0.1	1.5	316	72	658	1.717
4	KT315	65	0.1	1.5	295	132	622	1.605
5	KT315	80	0.1	1.5	281	130	601	1.41
6	KT315	100	0.1	1.5	277	130	598	1.667
7	KC9240	65	0.1	1.5	446	203	715	1.455
8	KC9240	80	0.1	1.5	441	184	694	1.368
9	KC9240	100	0.1	1.5	393	158	538	0.755
10	K313	65	0.15	1.5	398	96	919	3.649
11	K313	80	0.15	1.5	371	90	901	3.462
12	K313	100	0.15	1.5	325	78	854	3.137
13	KT315	65	0.15	1.5	358	177	863	2.669
14	KT315	80	0.15	1.5	356	179	855	1.88
15	KT315	100	0.15	1.5	335	177	830	3.132
16	KC9240	65	0.15	1.5	527	272	966	1.492
17	KC9240	80	0.15	1.5	446	187	696	1.405
18	KC9240	100	0.15	1.5	436	195	697	1.085

with the KC9240 cutting tool (0.1 mm/r constant feed rate).

3.2 Optimization with the Taguchi Method

In this part the optimization of the turning parameters was carried out in terms of the cutting forces with the Taguchi analysis. The importance order of the effects of each control factor on the turning forces was identified. For this purpose, the factors selected in the Taguchi experimental design and the levels of these factors are shown in **Table 7**. Taguchi's L18 2*1 3*2 mixed design was used. In the Taguchi method there are three categories, i.e., "the smallest is better", "the biggest is better" and "the nominal is better" for the calculation of the signal/noise (*S/N*) ratio. In this research "smallest is better" was used since the minimum of the cutting force and surface roughness was intended. In the *i*th experiment, the *S/N* ratio can be calculated using the following equation.[17–19]

$$\eta_i = -10 \log_{10} \frac{1}{n} \sum_{1}^{n} Y_i^2 \qquad (1)$$

n is the number of replications and Y_i is the measured characteristic.

Table 7: Cutting parameters and levels

Tabela 7: Parametri rezanja in nivoji

Control parameters		Units	Levels		
			1	2	3
Feed rate	(A)	m/min	65	80	100
Cutting speed	(B)	(mm/r)	0.1	0.15	
Cutting tool	(C)		KC313	KT315	KC9240

3.3 Confirmation Experiments

The final step of the Taguchi experimental design process includes confirmation experiments.[18,19] To achieve this, the results of the experiments were compared with the predicted values using the Taguchi method and the error rates were obtained. The *S/N* ratios were predicted using the following model:[18–20]

$$\eta_{\text{pred}} = \eta_m + \sum_{i=1}^{k} (\eta_i - \eta_m) \qquad (2)$$

Moreover, the optimum turning parameters were obtained for the performance characteristics using the Taguchi analysis, where m is the total mean of the *S/N* ratios, i is the mean *S/N* ratio at the optimum level and k is the number of the main design parameters that significantly affect the performance characteristics. After predicting the *S/N* ratios other than 18 experiments (with Eq.2), the main cutting force or F_z was calculated using the following equation:[20]

$$Y_{\text{pred}} = 10^{\frac{-S/N}{20}} \qquad (3)$$

where Y_{pred} is the main cutting force or F_z with regard to the *S/N* ratio.

3.4 Taguchi Analysis for F_z

Figure 4 shows the main effect plot for the *S/N* ratios, giving the effect of cutting parameters on the cutting force F_z. The smallest main cutting force is obtained with the cutting insert KT315. In this way, to achieve the minimum cutting forces it is understood that the KC9240 cutting tool should be used at a 0.10 mm/r feed rate and 100 m/min cutting speed.

After analysing the effect of the cutting parameters on the cutting force, in order to find out which F_z cutting force it effected, a variance analysis was made. According to the results of the ANOVA in **Table 8**, it is understood that the most effective cutting parameters that effected the cutting force was 65.99 % and the cutting speed was 11.14 %.

Table 8: ANOVA results for F_z
Tabela 8: ANOVA-rezultati za F_z

Source	DF	Sum of squares	Mean square	*F*	Prob > *F*	Distribution %
A	1	181805	181805	57.75	0.002	65.99
B	2	30700	15350	4.88	0.085	11.14
C	2	13213	6607	2.1	0.238	4.80
A*B	2	4024	2012	0.64	0.574	1.46
B*C	2	9391	4696	1.49	0.328	3.41
A*C	4	23792	5948	1.89	0.276	8.64
Error	4	12592	3148			4.57
Total	17	275517				100.00

3.5 Taguchi Analysis for R_a

Figure 5 shows the effect of feed rate, cutting speed and cutting-tool material on the average surface roughness. According to this figure, in order to obtain the smallest surface roughness, it is necessary to use the KC9240 cutting tool at a low feed rate (0.10 mm/r) and a high cutting speed (100 m/min). Besides this, in order to find out which important parameter affects the surface the roughness, the variance analysis was made with this aim. According to the results of the ANOVA in **Table 9**, the cutting parameters which effect the surface roughness, the cutting tool (40.38 %), feed rate, (33.15%) and 15.57 % feed speed and cutting tool's interaction were found.

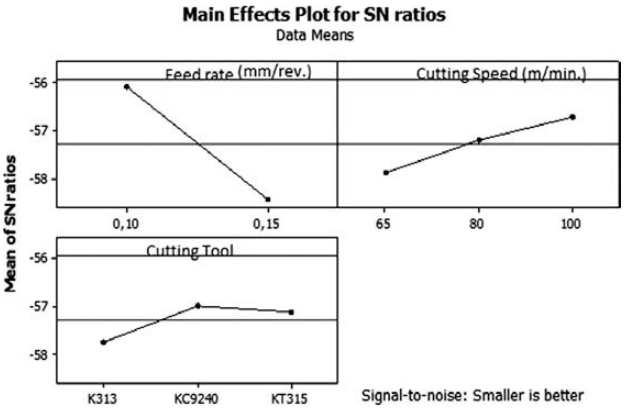

Figure 4: Mean response graphs of the cutting forces according to the feed rate, cutting speed and cutting tool
Slika 4: Prikaz odziva sil rezanja glede na hitrost podajanja, hitrost rezanja in rezilnega orodja

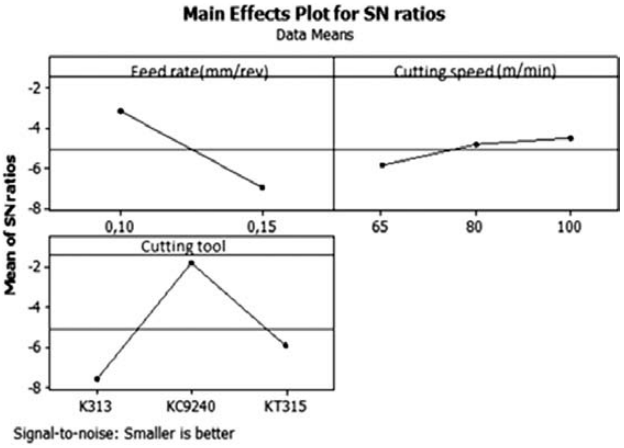

Figure 5: Mean response graphs of the surface roughness according to feed rate, cutting speed and cutting tool
Slika 5: Prikaz odziva hrapavosti površine glede na hitrost podajanja, hitrost rezanja in rezilnega orodja

Table 9: ANOVA results for R_a
Tabela 9: ANOVA rezultati za R_a

Source	DF	Sum of squares	Mean square	*F*	Prob > *F*	Distribution %
A	1	4.1424	4.1424	56.56	0.002	33.15
B	2	0.18817	0.09408	1.28	0.371	1.51
C	2	5.04646	2.52323	34.45	0.003	40.38
A*	2	0.06687	0.03343	0.46	0.663	0.54
B*C	2	0.81483	0.20371	2.78	0.173	6.52
A*C	4	1.94611	0.97305	13.29	0.017	15.57
Error	4	0.29294	0.07323			2.34
Total	17	12.49777				100.00

4 CONCLUSIONS

The goal of this study was to identify the effect of turning parameters such as feed rate, cutting speed and cutting tools on the main cutting force and surface roughness using an analysis of Taguchi. The experimental design described here was used to develop the main cutting force and the surface-roughness prediction model for the Hastelloy X turning operation. The results of this experimental study can be summarized as follows:

- The main cutting force decreased with increasing cutting speed and the cutting force increased at higher feed rates.
- According to the analysis of Taguchi, in order to obtain the smallest cutting force and surface roughness, it was necessary to use the KC9240 cutting tool

at a low feed rate (0.10 mm/r) and a high cutting speed (100 m/min).

- The minimum main cutting force is obtained with CNMG 120404-type multicoated TiN+AL_2O_3-TiCN+TiN carbide tools, while the maximum main cutting force is obtained as 965 N with the CNMG 120404-type uncoated carbide tools. However, cemented carbide tools have no significant effect on the main cutting force when machining Hastelloy X.
- An increasing relation between the cutting speed and the arithmetic average surface roughness as well as between the coating number and the average surface roughness is observed.
- In the case of coated tools, the effect of cutting speed on the surface roughness is no more pronounced than the effect of uncoated cemented-carbide inserts.
- The minimum average surface roughness is determined with CNMG 120404-type multicoated TiN+AL_2O_3-TiCN+TiN carbide tools, while the maximum average surface roughness is observed with CNMG 120404-type uncoated tools. Moreover, uncoated and multiple-layer coated tools have a significantly different effect on the average surface roughness.
- It was found that there is a positive correlation between the main cutting force and the average surface roughness.

Acknowledgments

The authors would like to express their gratitude to the University of Yuzuncu Yıl for the financial support Under Project No. BAP 2012-BYO-013.

5 REFERENCES

[1] Q. Zhang, R. Tang, K. Yin, X. Luo, L. Zhang, Corrosion behavior of Hastelloy C-276 in supercritical water, CSci., 51 (**2009**), 2092–2097

[2] V. B. Singh, A. Gupta, The electrochemical corrosion and passivation behavior of Monel 400 in concentrated acids and their mixtures, Transaction of JWRI., 34 (**2000**), 19–23

[3] Haynes Hastelloy C-22HS Standard Product Catalogue, Haynes International, Indiana, 2007, 2–16

[4] P. C. Jindal, A. T. Santhanam, U. Schleinkofer, A. F. Shuster, Performance of PVD TiN, TiCN, and TiAlN coated cemented carbide tools in turning, Int. J. Recfrac. Met. Hard Mater., 17 (**1999**), 163–170

[5] Website of trademark owner of Hastelloy C-276. www.hynesintl.com

[6] M. Wang, Ph. D. Thesis, South Bank University, London, 1997

[7] N. Richards, D. D. Aspinwall, Use of ceramic tools for machining nickel-based alloys, Int. J. Mach. Tools Manuf., 29 (**1989**) 4, 575–588

[8] E. O. Ezugwu, Z. M. Wang, Performance of PVD and CVD coated tools when machining nickel-based, Inconel 718 alloy, In: N. Narutaki, et al. (Eds.), Third International Conference on Progress of Cutting and Grinding, 111 (**1996**), 102–107

[9] H. Khamsehzadeh, Behaviour of ceramic cutting tools when machining superalloys, Ph.D. Thesis, Universtiy of Warwick, 1991

[10] J. Barry, G. Byrne, Cutting tool wear in the machining of hardened steels. Part I. Cubic boron nitride cutting tool wear, Wear, 247 (**2001**), 139–151

[11] B. M. Kramer, P. D. Hartung, Proc. Int. Conf. of Cutting Tool Mat., Fort Mitchell, KY, (**1980**), 57–74

[12] A. E. Focke, F. E. Westermann, A. Ermi, J. Yavelak, M. Hoch, Failure mechanisms of superhard materials when cutting superalloys, in: Proc. 4th Int.-Am. Conf. of Mat. and Tech, Caracus, Venezuela, 1975, 488–497

[13] W. Konig, A. Berktold, J. Liermann, N. Winands, Top quality components not only by grinding, Ind. Diamond Rev., 3 (**1994**), 127–132

[14] C. Çakır, Modern metal cutting principles, Vipaş, Bursa 2000

[15] Sandvik, Modern metal cutting practical Handbook, Sandvik 1994

[16] R. I. King (Ed.), Handbook of high speed mach., techn. Chapman and Hall, London 1985

[17] A. Taskesen, K. Kütükde, Optimization of the drilling parameters for the cutting forces in B4C-reinforced Al-7XXX-series alloys based on the Taguchi method, Mater. Tehnol., 47 (**2013**) 2, 169–176

[18] G. Tosun, Statistical analysis of process parameters in drilling of AL/SIC P metal matrix composite, International Journal of Advanced Manufacturing Technology, 55 (**2011**) 5–8, 477–485

[19] R. K. Roy, A primer on the Taguchi method / Ranjit K. Roy, Van Nostrand Reinhold, New York, 1990

[20] K. Palanikumar, Experimental investigation and optimization in drilling of GFRP composites, Measurement, Journal of the International Measurement Confederation, 44 (**2011**) 10, 2138–2148